Journal of Thermal Analysis, Vol. 37 (1991) 849-860

THERMAL DECOMPOSITION OF AMMONIUM METAVANADATE DOPED WITH Fe, Co OR Ni HYDROXIDES

*A. A. Said**

DEPARTMENT OF CHEMISTRY, FACULTY OF SCIENCE, UNITED ARAB EMIRATES
UNIVERSITY, AL-AIN, P O. BOX 17551, U. A. E.

(Received October 29, 1990)

The thermal decomposition of pure ammonium metavanadate (AMV) and of AMV doped with Fe^{3+},Co^{2+} or Ni^{2+} ions was investigated by TG, DTA, IR and X-ray diffraction. The results obtained revealed that the presence of these dopants enhances the formation of the intermediate compounds V_2O_5 solid. Some of the V^{5+} ions of the V_2O_5 lattice seemed to be reduced to V^{4+} ions. The activation energies of the different decomposition stages for all samples were calculated. The doped solids calcined at 450°C were characterized by the determination of S_{BET} and by electrical conductivity measurements. The mechanisms by which these ions affect the properties of the solids produced are discussed in relation to the defect structure created by the doping process.

The mechanisms of thermal decomposition of many solid substances involve a number of stages between the initial and final products [1–5]. It has been found [6–8] that these mechanisms depend mainly upon the atmosphere in contact with the solid. On the other hand, it has been observed by several authors that the doping of solids can markedly influene the reaction rate and activation energy of solid-phase reactions [2, 3–9]. The effect of doping has been attributed to a change in the defect structure of the reacting substances [10, 11]. The thermal decomposition of ammonium metavanadate (AMV) has been the subject of several investigations [3, 12–15]. It is known that AMV is very sensitive to the presence of different foreign substances [10], where the net solid products can be used effectively as catalysts [16]. However, the influence of Fe^{3+}, Co^{2+} and Ni^{2+} ions on the

---

* Permanent address: Department of Chemistry, Faculty of Science, Assiut University, Assiut, Egypt

John Wiley & Sons, Limited, Chichester
Akadémiai Kiadó, Budapest

thermal decomposition of AMV has received relatively little attention. The present investigation was devoted to a study of (i) the thermal decomposition of pure AMV and of AMV doped with Fe^{3+}, Co^{2+} or Ni^{2+} ions, and (ii) the characterization of the solid products obtained throughout the course of the thermolysis. The techniques employed were TG, DTA, IR, X-ray diffraction, surface area and electrical conductivity measurements.

Experimental

Materials

BDH "Analar" AMV was the starting material. AMV samples doped with Fe^{3+}, Co^{2+} or Ni^{2+} ions were prepared by adding the calculated amounts of $Fe(OH)_3$, $Co(OH)_2$ $Ni(OH)_2$ in proportions of 0.5, 1 and 5 mol% to AMV. The samples were admixed by using bidistilled water, evaporated, and then dried in an oven at 110° to constant weight.

Techniques

The thermogravimetric analysis (TG) and differential thermal analysis (DTA) of pure AMV, and the DTA of the various doped solid samples were carried out with a Shimatzu Computerized Thermal Analysis System DT–40. The system includes programs which process data from the thermal analyzer with the Chromatpac CR 3 A. The rate of heating of the samples was kept at 10 deg min^{-1}, in an air atmosphere. A 5 mg sample of each solid was employed in each case. Al_2O_3 calcined at 1300° was applied as a reference material.

The IR spectra of the thermal products of AMV were recorded from KBr discs, with a Pye–Unicam 2000 infrared spectrophotometer. The IR spectra were determined in the range 4000–250 cm^{-1}, but only the portion between 1500 and 250 cm^{-1} was considered in the present work.

The X-ray diffraction patterns of the thermal products of AMV were obtained by using the powder diffraction pattern technique at a value of 2θ between 2° and 60°, using a Philips Unit of type PW 2103, a Cu target and a Ni filter.

The specific surface areas of pure and doped AMV were determined by means of N_2 adsorption at −195°, with a conventional volumetric apparatus [17].

The electrical conductivity measurements were carried out with a method discussed previously [18].

Results and discussion

Thermal decomposition of ammonium metavanadate

Figure 1 presents the DTA and TG curves of undoped AMV. Three endothermic peaks are observed (curve a), with maxima at 203, 229 and 333°. The TG curve given in Fig. 1b shows that the original AMV loses weight in three steps when heated. The first peak, which was accompanied by an 11.7% loss in weight, indicated the decomposition of AMV to the intermediate ammonium bivanadate (ABV), according to

$$6[(NH_4)_2O\cdot V_2O_5] \xrightarrow{162-222^\circ} 3[(NH_4)_2O\cdot 2V_2O_5]+6NH_3+3H_2O \qquad (1)$$

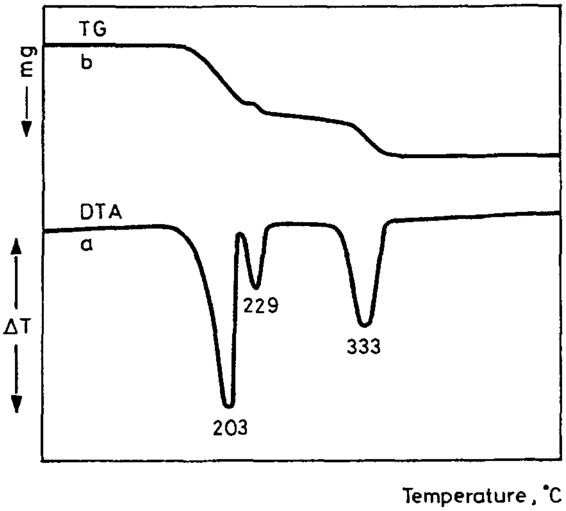

Fig. 1 DTA and TG curves of pure AMV

This was followed by the second decomposition stage, which was accompanied by a 3.6% loss in weight, indicating the decomposition of ABV to the intermediate ammonium hexavanadate (AHV), according to

$$3[(NH_4)_2O\cdot 2V_2O_5] \xrightarrow{225-245^\circ} 2[(NH_4)_2O\cdot 3V_2O_5]+2NH_3+H_2O \qquad (2)$$

The third peak, which was accompanied by a 7.8% loss in weight, corresponded to the decomposition of AHV to V_2O_5:

$$2[(NH_4)_2O\cdot 3V_2O_5] \xrightarrow{314-352^\circ} 6V_2O_5+4NH_4+2H_2O \qquad (3)$$

These results were found to be in agreement with the data reported by Brown *et al.* [15].

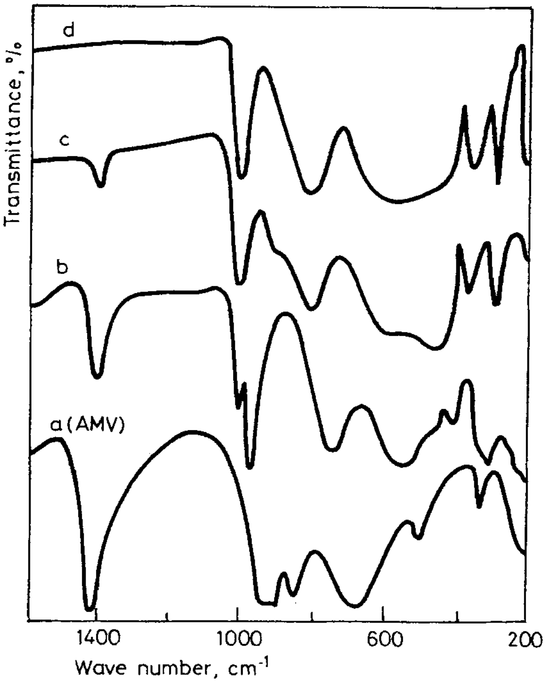

Fig. 2 Infrared absorption spectra for AMV (a) and its calcination products at 200 (b), 250 (c) and 450°C (d)

The IR spectra given in Fig. 2 relate to the products of calcination of the parent AMV at 200, 250 and 450° for 3 h in an air atmosphere. Curve b shows a decrease in the absorption intensity of the coordinated ammonium band at 1410 cm^{-1}. This indicates formation of the first intermediate (ABV). As the calcination temperature is increased to 250° (curve c), the further decrease in the intensity of the ammonium band indicates formation of the second intermediate (AHV). Calcination of AMV at 450° (curve d) indicates the complete disappearance of the absorption band at 1410 cm^{-1} and the formation of a V_2O_5 solid lattice. Moreover, the bands at 1020 and 840 cm^{-1} are assigned to the V = O and V – O – V stretching vibration bands [19, 20], respectively.

Different specimens of AMV were subjected to heating in an air atmosphere for 3 h at 250, 300 and 450°. From Fig. 3, the characteristic *d*–spacings and the corresponding relative intensities were compared with the standard ASTM cards [21]. The results show that the most intense lines correspond to the V_2O_5 solid lattice. However, the intensities of the diffraction lines were found to increase on increase of the calcination temperature.

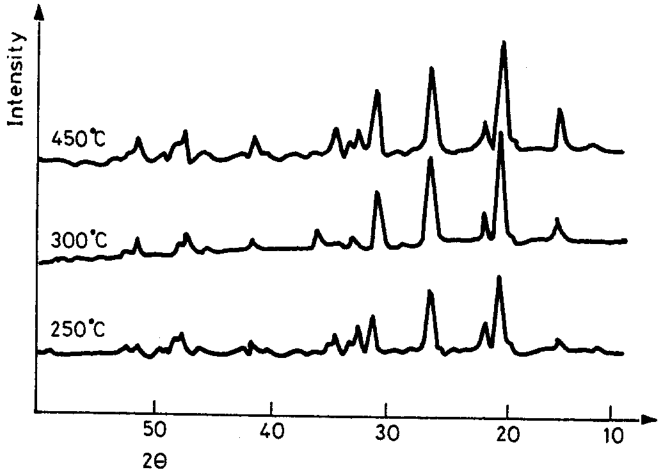

Fig. 3 X–ray diffraction patterns for the calcination products of AMV

Thermal decomposition of AMV doped with different proportions of Fe^{3+}, Co^{2+} or Ni^{2+} ions

Figures 4, 5 and 6 present the DTA curves of AMV and of AMV doped with 0.5, 1 or 5 mol% of Fe^{3+}, Co^{2+} or Ni^{2+} ions, respectively. The comparison of these latter curves with those for pure AMV reveals some trends and permits conclusions.

(i) All the dopant ions enhance the formation of the first intermediate (ABV), this enhancement increasing with increase of the dopant concentrations. The maxima of the decomposition temperatures for this stage are given in Table 1.

(ii) The second stage, involving the formation of AHV, exhibits different behaviour in the presence of the various dopants. In the case of Fe^{3+} ions, an enhancement of the formation of AHV is observed in the presence of 0.5 mol% Fe^{3+} ions. On further increase of the concentration of Fe^{3+} ions, a new exothermic peak is observed. The appearance of this peak at 240° or at 245° in the presence of 1 or 5 mol% Fe^{3+} ions, respectively, may be attributed to the conversion of ferrihydroxide to α-Fe_2O_3 [22]. The addition of 0.5 or 1 mol% Co^{2+} ions enhances the formation of AHV, while on the addition of 5 mol% Co^{2+} an exothermic peak appears. The appearance of this peak at 250° may correspond to the decomposition of $Co(OH)_2$ to Co_3O_4 [23]. In the presence of Ni^{2+} ions, a slight enhancement of the formation of AHV is observed. The new exothermic peak, located at 250°, corresponds to the decomposition of $Ni(OH)_2$ [24]. It is worthy of mention that all the dopants not only enhance the formation of AHV, but also decrease its peak area. This indicates that the addition of these dopants to AMV should retard the formation of AHV.

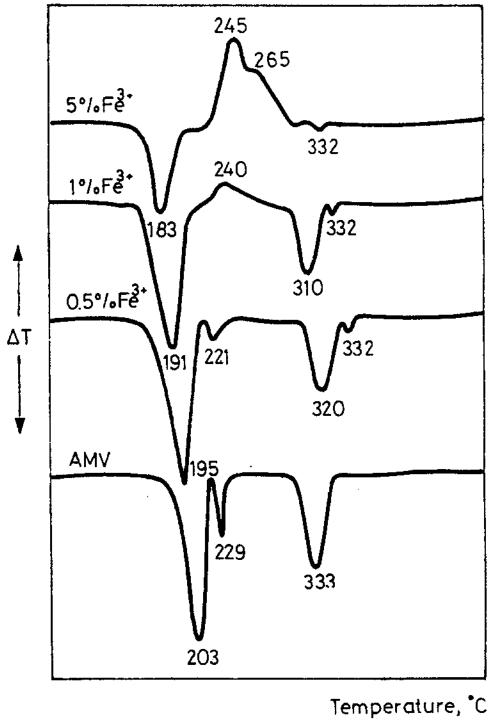

Fig. 4 DTA curves of pure AMV and doped with different proportions of Fe^{3+} ions

(iii) The third stage, involving the decomposition of AHV to V_2O_5, occurs at temperatures lower by 19-23 deg: in the presence of 1 mol% of Fe^{3+}, Co^{2+} or Ni^{2+} ions. The addition of 5 mol% of dopant causes the same effect as 1 mol% of Co^{2+} or Ni^{2+} ions, whereas for Fe^{3+} ions it causes a noticeable decrease in the decomposition temperature of the third stage. The exothermic peaks at 245 and 265° correspond to the decomposition of iron hydroxide together with AHV. The small endothermic peak at 332° in the DTA curves of all doped samples may be attributed to the formation of V^{4+}. In this step, some dopant ions could be dissolved in the V_2O_5 lattice, forming tetravalent vanadium ions according to the following mechanism:

$$Fe_2O_3 \rightarrow 2Fe|V|' + V_2O_4 + \frac{3}{2}O_2 \qquad (4)$$

$$2NiO \rightarrow 2Ni|V|''' + V_2O_4 + O_2 \qquad (5)$$

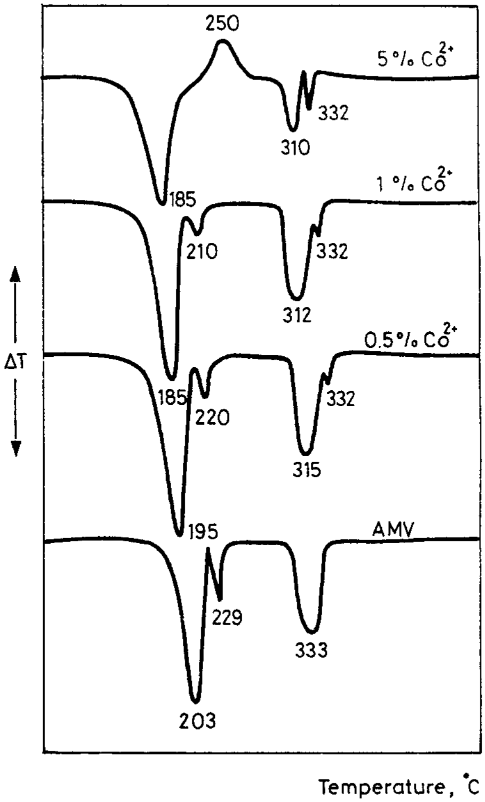

Fig. 5 DTA curves of pure AMV and doped with different proportions of Co^{2+} ions

It is known that Co_3O_4 is a spinel from CoO and Co_2O_3:

$$2CoO \rightarrow 2Co|V|''' + V_2O_4 + O_2 \tag{6}$$

$$Co_2O_3 \rightarrow 2Co|V|' + V_2O_4 + \frac{3}{2}O_2 \tag{7}$$

where $Fe|V|'$, $Ni|V|'''$, $Co|V|'''$ and $Co|V|'$ represent Fe^{3+}, Ni^{2+}, Co^{2+} and Co^{3+} replacing V^{5+} in its normal lattice position. From the above mechanisms, it appears that the amount of V^{4+} produced in the case of

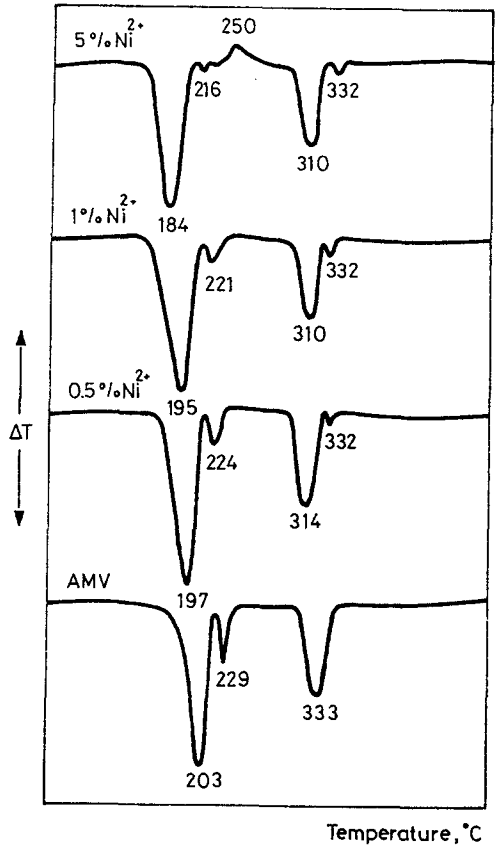

Fig. 6 DTA curves of pure AMV and doped with different proportions of Ni^{2+} ions

Co_2O_3 is greater than that produced in the cases of Fe^{3+} and Ni^{2+} ions. This is in accordance with the experimental results.

The calculated activation energies of the different decomposition stages of AMV and the doped samples are given in Table 1.

Table 1 E_a values (kJ/mol NH_4VO_3) and the maximum decomposition temperatures (°C) of AMV and AMV doped with Fe^{3+}, Co^{2+} or Ni^{2+} ions

Samples	1st stage		2nd stage		3rd stage		New peaks	
	Temp.	E_a	Temp.	E_a	Temp.	E_a	Temp.	E_a
AMV	203	−62.4	229	−5.5	333	−32.7	–	–
AMV+0.5% Fe^{3+}	195	−43.3	221	−4.0	320	−19.4	332	−0.5
AMV+1 % Fe^{3+}	191	−40.8	–	–	314	−13.3	240	+5.9
AMV+5 % Fe^{3+}	183	−17.2	–	–	–	–	245, 265	+33.6
AMV+0.5% Co^{2+}	195	−40.7	220	−2.5	315	−22.0	332	−0.5
AMV+1 % Co^{2+}	188	−38.1	210	−1.1	312	−21.0	332	−3.3
AMV+5 % Co^{2+}	185	−19.6	–	–	310	−13.4	248	+11.8
AMV+0.5% Ni^{2+}	197	−45.1	224	−3.2	314	−23.8	332	−0.5
AMV+1 % Ni^{2+}	195	−46.7	221	−2.2	310	−22.8	332	−0.6
AMV+5 % Ni^{2+}	184	−34.6	216	−0.4	310	−17.8	250	+5.3

It appears that the activation energies of the different stages of thermal decomposition of AMV are in agreement with the reported data [15]. Noticeable decreases occur in these values in the presence of the different additives. The magnitude of the activation energy has often been ascribed to the energy barrier in the rate-limiting step. Therefore, the presence of Fe^{3+}, Co^{2+} or Ni^{2+} ions may cause lattice deformations as well as holes [2] either on the surface or in the bulk, which in turn will strongly affect the thermal decomposition via the enhancement of the decomposition stages. Consequently, the doped samples should require a lower activation energy for thermolysis to be achieved. Additionally, the doping of AMV with 5 mol% Fe^{3+}, Co^{2+} or Ni^{2+} ions is the most effective according to the energy released.

It is known that the reactive solids produced during the thermal decomposition of AMV doped or mixed with foreign ions can be used as catalysts in many important reactions. However, to understand the catalytic behaviour of these catalysts, some physico-chemical experiments should be performed. Therefore, S_{BET} and the semiconducting properties of the solids produced were determined.

Surface area measurements

The specific surface areas of the thermal products of AMV and AMV doped with Fe^{3+}, Co^{2+} or Ni^{2+} ions, calcined at 450° for 3 h in an air atmosphere, were determined by applying the BET equation [25] in its normal range of applicability. The values of S_{BET} are listed in Table 2.

Table 2 S_{BET} of the thermal products of pure AMV and of AMV doped with Fe^{3+}, Co^{2+} or Ni^{2+} ions

Dopants	S_{BET}, $m^2 \cdot g^{-1}$			
	V_2O_5	0.5	1	5
Fe^{3+}	6.5	7.5	8.3	10.3
Co^{2+}	6.5	7.0	7.8	8.5
Ni^{2+}	6.5	8.0	9.7	12.2

The surface area of V_2O_5 increases with increasing dopant ratio. This increase generally results from the vanadium vacancies and holes created during the thermolysis of the original doped samples. This behaviour is well illustrated by the foregoing proposed mechanisms in the following electrical conductivity results.

Electrical conductivity measurements

The electrical conductances of the solids produced from the calcination of pure AMV and of AMV doped with Fe^{3+}, Co^{2+} or Ni^{2+} ions at 450° for 3 h in an air atmosphere were measured. The values of σ were measured at 250° in an air atmosphere with a flow rate of 200 $ml \cdot min^{-1}$. The values of log σ are depicted in Table 3.

Table 3 Variation in log σ with the amount of Fe^{3+}, Co^{2+} or Ni^{2+} ions

Dopant	log σ			
	V_2O_5	0.5	1	5
Fe^{3+}	–4.6	–5.2	–5.4	–5.8
Co^{2+}	–4.6	–5.4	–5.9	–6.7
Ni^{2+}	–4.6	–5.1	–5.5	–6.0

The above results show a decrease in the conductance of V_2O_5 on increase of the concentration of dopant. This behaviour would be expected since the doping of V_2O_5 will decrease the charge carrier concentrations through oxygen chemisorption according to the following mechanism:

$$O_2 + Fe_2O_3 \rightarrow 2\mathrm{Fe}|\mathrm{V}|'' + V_2O_5 + 4|e|^{\cdot} \qquad (8)$$

$$\frac{3}{2}O_2 + 2NiO \rightarrow 2\mathrm{Ni}|\mathrm{V}|''' + V_2O_5 + 6|e|^{\cdot} \qquad (9)$$

$$O_2 + Co_2O_3 \rightarrow 2\mathrm{Co}|\mathrm{V}|'' + V_2O_5 + 4|e|^{\cdot} \qquad (10)$$

$$\frac{3}{2}O_2 + 2CoO \rightarrow 2\mathrm{Co}|\mathrm{V}|''' + V_2O_5 + 6|e|^{\cdot} \qquad (11)$$

where $\mathrm{Fe}|\mathrm{V}|''$, $\mathrm{Ni}|\mathrm{V}|'''$, $\mathrm{Co}|\mathrm{V}|''$ and $\mathrm{Co}|\mathrm{V}|'''$ represent Fe^{3+}, Ni^{2+}, Co^{3+} and Co^{2+} cations occupying V^{5+} sites in the V_2O_5 lattice, and $|e|^{\cdot}$ is a defect electron. From the above mechanisms, it appears that the concentration of charge carriers decreases in the sequence iron < nickel < cobalt ions. Moreover, these mechanisms agree with the experimental results. It is important to mention that the creation of electron defects should decrease the *n*–type character of V_2O_5.

References

1 M. E. Brown, D. Dillmore and A. K. Gallwey, Reactions in the solid state, (C. H. Banford and C. F. H. Tippaer (Eds.)) Vol. 22, Comprehensive Chemical Kinetics, Elsevier, Amsterdam 1980.
2 A. A. Said, K. M. Abd El-Salaam and E. A. Hassan, Surf. Technol., 19 (1983) 241.
3 E. A. Hassan, A. A. Said and K. M. Abd El-Salaam, Thermochim. Acta, 96 (1985) 219.
4 G. A. El Shobaky, K. A. El-Baraway and F. H. A. Abdulla, Thermochim. Acta, 96 (1985) 129.
5 A. A. Ibrahim and G. A. El-Shobaky, Thermochim. Acta, 147 (1989) 175.
6 L. N. Koval, V. S. Muzykantov, L. V. Kurina and G. K. Boreskov, Kinet. Katal., 15 (1974) 1193.
7 R. Gajerski, S. Komornicki, A. Malecki and A. Podgoreck, Mater Chem., 4 (1979) 135.
8 S. A. Selim and C. A. Philip, Thermochim. Acta, 39 (1980) 267.
9 K. M. Abd El-Salaam and E. A. Hassan, Surf. Technol., 11 (1980) 55.
10 K. M. Abd El-Salaam and A. A. Said, Surf. Technol., 17 (1982) 194.
11 F. Solymosi and Z. G. Szabó, J. Chem. Soc., (1961) 2745.
12 V. V. Popovski, E. A. Mamedov and G. K. Boreskov, Kinet. Katal., 13 (1972) 145.
13 L. M. Koval, V. S. Muzkantov, L. N. Kurina and G. K. Boreskov, Kinet. Katal., 15 (1974) 1193.
14 T. M. Sas, V. A. Novozhilon and Y. A. Velikodnyi, Zh. Neorg. Khim., 23 (1978) 3254.
15 M. E. Brown and B. V. Stewart, Thermal Anal. Vol. 2, Proc. 3rd ICTA Davos 1971, p. 313.
16 B. S. Milisovlevich, A. A. Ivanov, G. M. Polyakova and V. V. Serchantova, Kinet. Katal., 16 (1975) 103.
17 J. H. DeBoer, "The Dynamical Character of Adsorption", Clarendon Press, Oxford 1953.
18 K. M. Abd El-Salaam and A. A. Said, Surf. Technol., 17 (1982) 199.
19 K. Huffe and K. M. Abd El-Salaam, Ber. Bunsenges. Phys. Chem., 82 (1978) 1321.
20 Y. Kera and K. Hirota, J. Phys. Chem., 73 (1969) 3973.
21 American Society for Testing Materials: X-ray Powder Data File Ed. J. V. Smith, Philadelphia 1960.
22 S. V. S. Prasad and V. Sitakaru Rao, J. Mat. Sci., 19 (1984) 3266.

23 M. Figlarz, J. Guenot and J. N. Tournemolle, J. Mat. Sci., 9 (1974) 772.
24 R. B. Fahim, R. M. Gabr, M. I. Zakai and A. A. Mansour, Surf. Technol, 17 (1982) 175.
25 S. Brunauer, P. H. Emitt and E. Teller, J. Amer. Chem. Soc., 59 (1938) 1533.

Zusammenfassung — Mittels TG, DTA, IR und Röntgendiffraktion wurde die thermische Zersetzung von reinem Ammoniummetavanadat (AMV) und von AMV, versetzt mit Fe^{3+}, Co^{2+} oder Ni^{2+}, untersucht. Die Ergebnisse zeigen, daß die Bildung von Zwischenprodukten und festem V_2O_5 durch die Gegenwart der Zusätze begünstigt wird. Einige der V^{5+}-Ionen des V_2O_5 Gitters scheinen zu V^{4+}-Ionen reduziert zu sein. Für alle Proben wurde die Aktivierungsenergie der verschiedenen Zersetzungsschritte berechnet. Die versetzten Feststoffe, die bei 450°C kalziniert wurden, konnten durch die Bestimmung von S_{BET} und durch elektrische Leitfähigkeitsmessungen charakterisiert werden. Der Mechanismus, über welchen diese Ionen die Eigenschaften der Feststoffe beeinflussen, wurde hinsichtlich der hervorgerufenen Defektstruktur diskutiert.